5

Targeted Drug delivery of nanomedicines

Ayesha Sani[1], Dilawar Hassan[1], Sadia Mughal[2], Ahmed El-Mallul[3,4]

[1]Tecnologico de Monterrey, School of Engineering and Sciences, 52926, Atizapan de Zaragoza, Mexico
[2]Department of Medicine, Bahria University Medical and Dental College (BUMDC), Bahria University, Karachi
[3]Lodz University of Technology, Lodz, Poland
[4]Medical Department, University of Al Zintan, Al Zintan, Libya

Outline

Introduction

Traditional medicines and their defects Considering the escalating prevalence of diseases and disorders, there has been a growing recognition of the pivotal role played by targeted dosage forms in the realm of effective treatment and overall improvement of patient well-being. Traditional drug molecules don't contain selectivity for specific diseases cells, due to that there is a necessity for considering dosage and frequency of dosage. This can lead to serious harmful effects over the organisms. Traditional drugs have compromised effectiveness due to poor solubility, as they don't pass through the biological barriers. Consequently, the necessity grows to make insoluble drugs soluble and permeable through biological barriers. Traditional methods were not well effective so that there was always a need of drug administration again and again, lack of patient involvement, very short half-life, difficult to keep consistent drug concentration in blood plasma. It impedes attainment for drug delivery including target release, stable concentration in plasma, and low requirement of dosage. Therefore, a shift was taken to modify the drug delivery and drug release advanced methodologies for site specific drug delivery, intensify patient compliance as well as low requirement of drug intake.

Traditional drug molecules don't contain selectivity for specific diseases cells, due to that there is a necessity for considering dosage and frequency of dosage. This can lead to serious harmful effects over the organisms. Traditional drugs have compromised effectiveness due to poor solubility, as they don't pass through the biological barriers. Researchers also concluded that incorporating natural products or extracts in the form of drugs (orally or applicable), and into various conventional formulations, it proves to be beneficial to provide minimal therapeutics side effects. The natural products such as curcumin [1, 2], cinnamic acid [3], Luteolin [4], naringenin [5], etc., also enhanced the biological activity of various materials. The main challenge associated with these products is the large sized molecules, leading to inadequate bioavailability and absorption, poor solubility, in vivo instability. This addressed issue can result difficulty to introduce the natural products in pharmaceutical drugs.

Nanomaterials are considered as a material with diverse applications based on their size and shape. The material owing the capacity to use in various applications by altering its size. Furthermore, the structure of nanomaterials also plays important role in manipulating the properties of nanomaterials. New avenues of properties were highlighted when the surface plasma resonance of noble metals and band gap of semiconductors were modulated. The size and shape of the nanomaterial revealed the Catalytic properties and optical characteristics of noble metals also followed other tractable applications. Nanomedicine is the science which encloses the technology for treating, preventing, diagnosing, and monitoring diseases. Initially, it only used to enhance human health. In contrast, recently it has great potential to employs molecular tools, help to insight human body, capturing images as well as treating tumor. Beyond tumor, nanomedicines gave diverse field of applications for the treatment of ophthalmic diseases, gene editing, immunotherapy, neurological disorders, anti-infection. The key focus to introduce nanomedicines in biological field seems to be achieved. Drugs entrapped in nanomaterials which offers target delivery and reduce the harm to healthy cells. Therefore, the innovative formulation of nanomedicines improves the bioavailability, facilitates time dependent drug release, lower the drug dosage and extend the half-life of drug [6-8]. In the modern era, more than 50 nanomedicine formulation has been approved for clinical purpose as shown in Fig 5.1-5.2. These marketed formulations cover various medical areas, such as anesthesia, fungal treatment, infection control, iron-replacement, cancer and tumor treatments and so on [9].

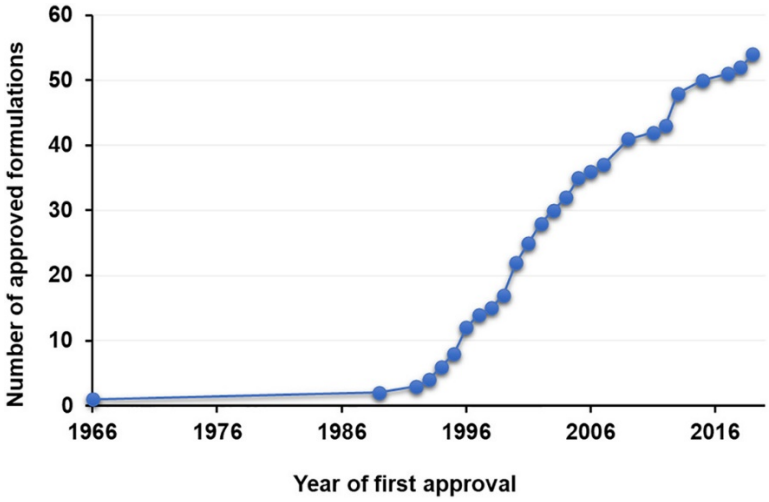

FIGURE 5.1
Approved formulations of drug from 1966-2016 [9].

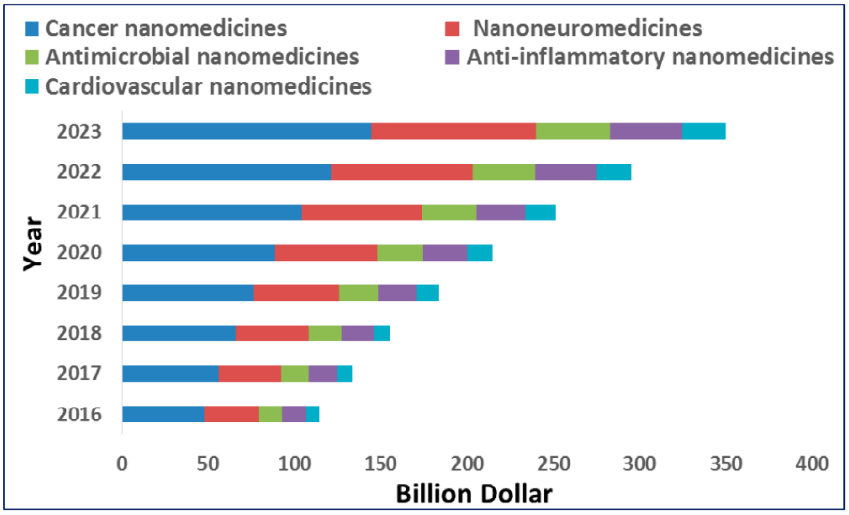

FIGURE 5.2
Illustration of worldwide nanomedicine market revenue from 2016-2023 [10].

Nanomaterial with functionalities

Surface modification is considered as the most compelling method to address and attenuate problems related to NPs toxicity. The surface modification or functionalization is a technique to closely linked different compositions including proteins, liposomes, nanocrystals, nano emulsions,

drugs, etc [11]. Nanomaterials can enter the body through various routes, including respiratory exposure, skin contact, ingestion, and injection. Once nanomaterials get inside the body it travels to organs and exerts biological effects such as cellular apoptosis, oxidative stress, inflammation, and DNA damage. To avoid these harmful effects, nanomaterials can be functionalized or modified with different bioactive molecules to reduce its harmful effects and enhance its characteristic properties including controlled, sustained therapeutical effects. Pharmaceutical products can be dissolved, trapped, encapsulated, adsorbed, or attached to NPs. NPs were successfully used as a carrier to deliver hydrophobic and hydrophilic drugs or compounds, biological macromolecules, various proteins, and different types of vaccines. Various research demonstrated that NPs is also suitable for intravenous administration, turn more beneficial as compared to large microparticles [12]. Moreover, the composition of nanomaterials can be tailored using doping strategies previously applied to bulk materials or by constructing core–shell structures with layers featuring entirely different chemical frameworks. The focus in the advancement field was aimed to introduce surface functionalities to improve and enhance capabilities of nanomaterials. The technique of functionalization can change the optical characteristics by reducing the aggregation of nanomaterials. The modification of surface charge enables the recognition of binding with molecules or ions. The role of surface coatings on NPs is pivotal in propelling nanotechnology toward various applications [13].

Multifunctionalities

Currently, new generation is arising where surface of nanocarrier can exhibit multiple functionalities simultaneously. New avenues have opened up in the biomedical discipline and tissue engineering, food processing and packaging, and drug delivery system by integration of NPs with polymer sciences. Nanomaterials or smart polymers offer various advantages, including ease of synthesis and characterization, stable and reproduceable, high surface-to-charge ratio, non-immunogenicity, and various absorption properties. These qualities make them highly appealing as easy carrier of drug delivery and cost-effective formulations. The transition from macro- to nano-drug delivery systems involves controlled drug release targeted at particular sites, distinguishing them from less targeted conventional drug delivery systems. The synthesis of nano-drug delivery system was tailored based on the targeted organs and body parts. NPs are widely employed in drug delivery due to their versatile surface modification capabilities as shown in Fig 5.3. This property allows for easy customization to achieve desired effects, including biocompatibility, enhanced or prolonged drug release, and specific targeting, depending on the functional group present on the NPs surface. The properties of NPs itself can be alter, enhanced or reduced by conjugating or coating NPs with various molecules. For the development of nanomedicines, there are two more crucial factors are biocompatibility and degradability. These factors considered very important for DNA transporting, drugs and proteins. A systematic flow across the cell membrane can be ensured by surface to charge ratio and size of polymer NPs. Surface functionalization of NPs is a crucial methodology designed to enhance and introduce new properties that are beneficial for medical applications. Various nanomaterials exhibit definite chemical properties and functional groups on their surfaces, which serve as the starting points for functionalization. Generally, NPs surface modification initially involves homo or hetro functional groups or cross linker. These cross linkers are employed to introduce organic functional groups (such as R-NH2, R-COOH, etc.) on the surface, making them conducive to binding with biological molecules [11].

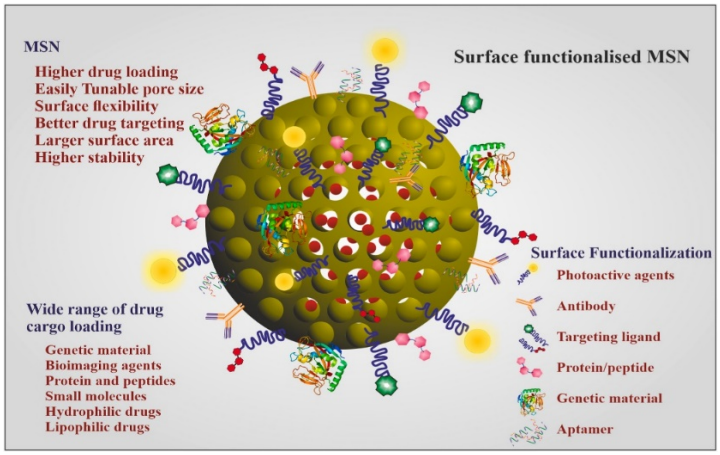

FIGURE 5.3
Illustration of various surface functionalized molecule [14].

Polymer

Polymers have extensive applications in biomaterials, which contains catalysis, biosensors, biocompatibility, biomimetic and drug delivery. In pharmaceutical, polymers becomes a valuable approach. Polymers exhibits significant benefits by maintaining drug stability, enhance efficacy, act as targeted therapeutic agents. Polymeric in the nanoscale range, are used to transport drugs. These polymeric NPs basically represent the conjugation of polymer with hydrophobic core encapsulating with specific drug of interest and surrounded by a hydrophilic coating [15]. Various natural polymers such as CS, polysaccharides, and synthetic polymers are used for drug delivery systems including PLGA (poly(dl-lactide co-glycolide)), PEG (poly(ethylene glycol)). Polymeric NPs also tuned with different functional groups to get better efficacy. PEG is a nontoxic, biocompatible material which shows antifouling properties. PLGA is a synthetic polymer, and easily undergoes hydrolysis inside the body [16].

Lipids, Carbon and Silicones

Liposomes have successful clinical trials for cancer therapy. Liposomes have amphiphilic nature hydrophilic heads and hydrophobic tails, therefore it carries both hydrophobic and hydrophilic drugs. This versatility makes liposomes valuable in the evolution of successful drug delivery system. Liposomes has bilayer phospholipid structure which provides a platform for encapsulating different therapeutic agents. Liposome possess many advantages including low immunogenicity, high biocompatibility, decreased toxicity, ease in change of shape and size [17]. Silicon coatings are biocompatible, increases the solubility of NPs whereas it doesn't affect the chemical properties, also provides stability to particles in changing environmental conditions [18]. Carbon provides the base for life. It provides different chemical bonds with different orientations. Carbon also possesses allotropic forms including graphite and diamond. Carbon has various forms, such as multiwalled carbon, nanotubes, nanorods, fibers, fullerenes, etc [19, 20].

Biomolecules

Bioactive compounds are the nature-based products, which exhibits unique properties for the useful treatment effects including antioxidant [21], antimicrobial [22], antispasmodic [23], antitumor [24], anti-inflammatory [25], etc. Curcumin is a bioactive compound which is yellow colored. Curcumin isolated from rhizomes of turmeric. Curcumin exhibits a range of pharmacological and physiological properties against chronic diseases. Gelatin is a compound which obtained from structural and chemical degradation of collagen. Gelatin has both acidic and basic functional groups therefore it can be available for both hydrophilic and hydrophobic compounds. Alginate is a basic natural copolymer which is biocompatible in nature. Alginate is linear polysaccharide and usually used in the form of hydrogels, microparticle, porous scaffolds, and NPs [26].

Various types of surface functionalization

Polymer functionalization

The study by Ayyanaar, S., et al, introduces a ROS (sensitive reactive oxygen) - responsive system incorporating LEC (lecithin) and Fe_3O_4, demonstrating anti-inflammatory capabilities. When the antioxidant drug CUR is encapsulated in PLGA hybrid magnetic microsphere system (Fe_3O_4@LEC-CUR-PLGA-MMS), the system becomes more efficacious. In H_2O_2 environment, ROS initiates the delivery system to facilitates release of payload CUR. Fe_3O_4@LEC-CUR-PLGA-MMS exhibits enhanced cell death against A549 and HeLa S3 cells with IC50 values. A549 cancer cell lines used 10 µg/mL and HeLa S3 cancer cell lines used 12 µg/mL. The system demonstrates superior in vitro cytotoxicity, induces changes in morphological structures, and limits colony formulations in HeLa S3 and A549 cancer cell lines compared to healthy cells. FTIR analysis of Fe_3O_4@LEC-CUR-PLGA-MMS confirms the characteristics bands of Fe_3O_4 NPs, Fe_3O_4@LEC NPs, PLGA and pure CUR, corresponding to functional groups in IR spectra. XRD analysis elucidates the crystallinity of Fe_3O_4@LEC-CUR-PLGA-MMS, indicating successful formation. TEM shows the spherical surface morphology with an average crystal diameter of 0.2 µm for Fe_3O_4. It also confirms the successful incorporation into the polymer as shown in Fig 5.4. Fe_3O_4@LEC-CUR-PLGA-MMS exhibits pH responsive ROS triggered, Release of CUR in acidic medium around pH of 5.4 and basic medium around pH of 7.4. MTT assays, fluorescence staining, and colony formation assays indicate that Fe_3O_4@LEC-CUR-PLGA-MMS act as an anticancer agent, it maintains cytocompatibility with healthy cells whereas showed toxicity to cancerous cells. In summary, this study presents an ROS responsive drug release mechanism that efficiently delivers therapeutic agents to disease sites, enhancing therapeutic efficacy for biomedical applications [27]. The research was conducted by Mansourizadeh, F., et al., to enhance medicinal efficacy of Salvigenin by designing mPEG-b-PLGA coated Fe_3O_4 NPs loaded with Salvigenin (Sal loaded PLGA@ Fe_3O_4 NPs). Physical and chemical properties were characterized using TGA, DLS, TEM. TEM micrographs confirmed that NPs had a uniform spherical size and shape. TEM images also showed dark regions corresponded to Fe_3O_4 NPs incorporated into mPEG-b-PLGA. These NPs have the average size around 57.4 ± 2 nm, whereas size distribution value was PDI= 0.168 ± 0.03. The surface charge of mPEG-b-PLGA@ Fe_3O_4 have a negative charge with zeta potential value −33 ± 1.2 mV. In vitro drug release profiles, drug loading, and entrapment efficiency were measured. Apoptotic detection test was done to confirm the anticancer activity of prepared NPs on MCF7 and MDA-MB-231 human breast cancer

cell lines. Salvigenin was successfully encapsulated in mPEG@-b-PLGA@Fe_2O_3 NPs with an efficiency of 82 ± 1.6%, and the NPs exhibited sustained release in phosphate buffer. The results of MTT assay revealed significant decrease in MDA-MB-231 and MCF7 cell viability with IC_{50} concentrations of 99.4 ± 1.7 µM and 74.2 ± 0.8 µM, respectively. Annexin V/PI analysis and cell cycle arrest at the Sub-G1 stage was confirmed by apoptosis. The results of western blot analyses revealed of an upregulation of Bax and a downregulation of Bcl_2 and Caspase-3 expression in the treated cells. Sal-loaded mPEG-b-PLGA@Fe_3O_4 NPs showed superior anticancer activity in breast cancer chemotherapy, suggesting their potential as a treatment option for various types of cancer [28]. Ahmed, A., et al., conducted a research in which $FeCl_3.6(H_2O)$ was used as the metal cluster and 2-aminoterephthalic acid (NH_2-BDC) as the organic linker (referred to NH_2-Fe-BDC) to synthesized dual-responsive iron-based metal-organic frameworks (MOFs). These MOFs were loaded with DOX (an anticancer drug). Further functionalization with PEG-FA (polyethylene glycol-folate) resulted in PEG-FA-NH_2-BDC. Folate moiety was incorporated to allow specific targeting of cancer that revel overexpression of the folate receptor. Techniques used to characterize material including DLS, XRD, FTIR and TGA were employed. Crystallinity of the NPs was validated through XRD pattern whereas, FTIR confirmed the conjugation of PEG-FA to the MOFs. Thermal stability of the MOFs was demonstrated by TGA. FTIR confirmed the conjugation of PEG–FA to the MOFs, and XRD patterns validated the crystallinity of the NPs. TGA results demonstrated the thermal stability of the MOFs. DLS results revealed that MOFs had a particle diameter of 577 nm, whereas improved colloidal stability with particle diameter of 461 nm was revealed for PEG-FA-functionalized MOFs. DOX entrapped efficiency was ~97% with an encapsulation capacity of around 14.5%. In vitro release profile studies revealed that under pH values (5.3 and 7.4) with or without frequency ultrasound, demonstrated the sonosensitivity of the nanovehicles. At pH 5.3, US-triggered release efficiency reached up to 90% after 280 min. MTT indicated that the synthesized material exhibited negligible toxicity effects at lower concentrations whereas higher concentrations shows more toxic effects. Cellular uptake was also studied via flow cytometry. The results demonstrated that the cellular uptake by cancer cells, increased with the conjugation of PEG-FA moiety to the MOF surfaces. Overall, this research highlighted the pH/US dual-responsive capability of PEG-FA-NH_2-Fe-BDC and NH_2-Fe-BDC act as smart drug delivery system [29]. Sampath, M., et al., discussed the bioavailability of CUR was enhanced through the use of PLGA (60/40) NPs, employing various capping agents such as CS, PEG and Dextrin, as well as the emulsifier Tocopherol Poly(Ethylene Glycol)1000 Succinate (TPGS). The method, emulsion solvent evaporation was employed for the synthesis of NPs, and the resulting NPs underwent thorough characterization. The zeta potential values depend on many factors including surface capping agents and with or without surface modification TPGS emulsified NPs exhibited a potential of 32.02 mV. The zeta potential values of particles were obtained without TPGS emulsification for CCPLGA NPs, DCPLGA NPs, and PCPLGA NPs, at 7.94 mV, 34.37 mV and 23.74 mV, respectively. Moreover, zeta potential values with TPGS emulsification were observed at TCCPLGA NPs= 32.14 mV, TDCPLGA NPs= 40.09 mV, and TPCPLGA NPs= 40.47 mV. Furthermore, it was also assumed that particle size reduced when positive zeta potential increased. As the capping agents change with TPGS emulsifier, simultaneously the contact angle varies for different capping agents. The water contact angel values for dextran, PLGA and CS coated CUR loaded PLGA NPs showed 79.5° ± 1.30, 55.6° ± 0.32, and 75.6° ± 2.57, respectively. The CUR loaded PLGA NPs showed water contact angel values ranged from 31 to 79°. Encapsulation efficiency and antioxidant activity of CUR by PLGA NPs also varies with different capping agents along with emulsifier TPGS such as Dextran, PEG and CS ranged from 82-89 % and 80 %, respectively. PLGA NPs embedded with CUR and different capping agents were used for in vitro studies which indicated

more enhanced effectiveness in inhibiting cell growth. After 24 h incubation, CUR-loaded PLGA NPs exhibited higher apoptotic potential, with this, these formulation TDPLGA NPs, TCPLGA NPs, and DCPLGA NPs showed higher therapeutic potential in MCF-7 cell lines. As compared to free CUR or other tested compounds, TDCPLGA NPs and TPCPLGA NPs showed higher apoptosis potential at IC_{50} concentration in MCF-7 cells. PLGA NPs with other capping agents, free CUR and emulsifier showed less cellular uptake than TPGS emulsified dextran-capped CUR encapsulated PLGA NPs [30]. PEG-modified thiolated gelatin (PEG-SHGel) NPs were synthesized by Kommareddy, S. and M. Amiji, to achieve various benefits in medical field such as passive targeted delivery responsive to intracellular glutathione concentrations, long-circulating system, enhanced and improved DNA delivery as well as transfection. Encapsulation of plasmid expressing enhanced green fluorescent protein (EGFO-N1) was done in NPs. The sized range for SHGel and Gel (DNA-containing gelatin) was approximately around 200 to 250 nm. After surface modification with PEG, the size range increased up to 310 to 350 nm. Electron spectroscopy for chemical analysis confirmed the PEG modifications, which showed the enhancement in ether peak intensities of the C1s spectra indicated the surface residues presence of ethylene oxide. PEG-SHGel NPs have the ability to release entrapped plasmid DNA (up to 5.0 mM GSH in phosphate-buffered saline) in response to different concentrations of glutathione. Agarose gel electrophoresis confirmed the presence of entrapped DNA stability. Murine fibroblast cells (NIH3T3) were chosen for In vitro studies which concluded that PEG-Gel and PEG-SHGel NPs consists greater transfection efficiency for the reported plasmid. Therefore, the research concluded that PEG-modified SHGel NPs have capability to serve as highly efficient nanoparticulate vectors for DNA delivery towards tumors. Moreover, cells have significantly higher intracellular GSH concentrations [31]. Norouzi, M., et al., studied, the antibiotic salinomycin, known for its anticancer properties, was encapsulated in magnetic IONPs to create a drug delivery system for potential glioblastoma (GBM) chemotherapy. The resulting Sali-PEI-PEG-IONPs were characterized, revealing size around 84.1 ± 14 nm and the zeta potential value +27.14 mV. TEM micrographs showed quasi-spherical shaped NPs with a size of 4.76 ± 0.7 nm. Polyethylenimine(PEI)-PEG-IONPs is a biocompatible material, which showed efficient uptake in human U251 GBM and mouse brain-derived microvessel endothelial (bEnd.3) cell lines. Sali-PEI-PEG-IONPs exhibited sustained salinomycin release over 4 days, with increased release in acidic pH. U251 cell proliferation was treated with Sali-IONPs, which showed the inhibition of U251 cells. Sali-IONPs reduced cell viability around 70% in 48 hours and instigate reactive oxygen species-mediated GBM cell death. Gene expression research demonstrated activation of caspases and modulation of various genes associated with cell cycle regulation and tumor suppression. In vitro studies showed that Sali-IONPs showed little penetration through the bEnd.3 monolayer in blood-brain-GBM co-culture model. However, when combined with an external magnetic field and hyperosmotic disruption, the permeability significantly increased, whereas, the viability decreases around 38% for U251 cells. Research study concluded that an effective and site-specific magnetic targeting can achieved for GBM chemotherapy by Sali-IONPs combined with penetration enhancer like external magnetic fields and hyperosmotic mannitol [32].

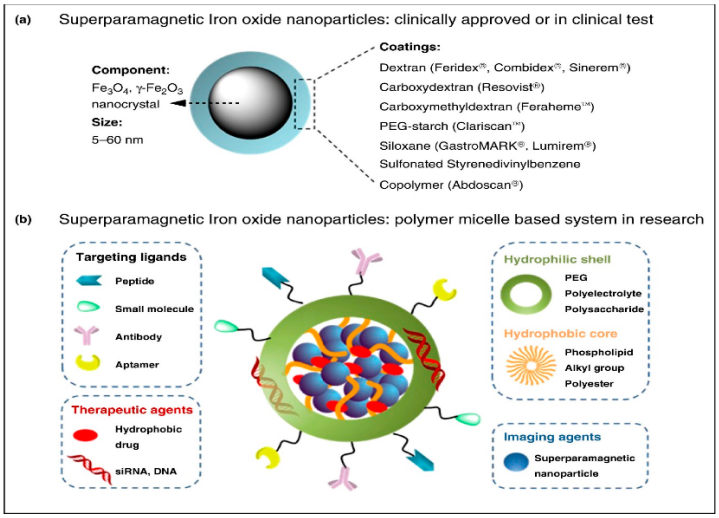

FIGURE 5.4
Schematic representation of Iron oxide with various Polymer, ligands, therapeutic agents [33].

Lipid functionalization

For drug delivery system, liposomes have unique physical and chemical stability including size distribution, minimal degradation and entrapment efficiency. Liposomes has unique physicochemical properties due to which it can circulate in blood for a longer time. Liposomes are the first nanomedicines which undergoes in clinical trials such as Doxil© and ABisome© [34]. Sintov, A.C., conducted research on, ALNs (Amylolipid nanovesicles, novel lipid modified starch molecules NPs, were synthesized for intranasal delivery of CUR to target the CNS (Central nervous system). The NPs were designed to address the challenges associated with the lower bioaccessibility and fast clearance of CUR, despite its potential therapeutic applications in CNS disorders. The data revealed that the ALNs, with or without crosslinked starch, exhibited a mean size between 130 and 150 nm in diameter, indicating a homogenous dispersion system with monodisperse characteristics. Polydispersity index values (0.11–0.20) confirmed the uniformity of the NPs dispersion. CUR is known for its therapeutical activities, such as the potential treatment of traumatic brain injury, brain tumor, central nervous system disorders like Alzheimer's disease. However, its bioavailability and clearance limitations hinder its therapeutic effectiveness. The study employed an optimized formulation of curcumin-loaded ALNs with 2% crosslinked starch, resulting in favorable brain and plasma concentrations. Following intranasal administration of this formulation at a dosage of 160 µg/kg, average quantity of CUR was found out in the brain was around 141.5 ± 55.9 ng/g, while the plasma concentration was 11.9 ± 12.0 ng/ml after one hour. In contrast, intravenous administration of the same dose did not lead to detectable CUR levels in the brain, while plasma concentration was almost half of that observed with intranasal ALNs. These results highlight the potential of well-designed ALN formulations as promising carriers for brain targeting and intranasal delivery, addressing challenges associated with its bioavailability for CNS applications [35]. In this study Boni, A., et al., synthesized oleic coated IONPs through thermal decomposition method with separate nucleation and growth

phases, as initially described by Hyeon et al. The chemical bonding was occurred between the carboxylic acid group with the metal iron center for the synthesis of oleic acid NPs. Modified C12-PAMAM dendrimer was applied as coating to disperse water repellent NPs in water, as reported by a novel method. The stable and highly concentrated water dispersion of NP allow most favorable characteristics as negative contrast agents. The study also explained the simultaneous conjugation of various functionalities to the PAMAM-coated NPs using fluorescent molecules. The coating and dissolution procedures were conducted under mild conditions due to the prevention of structural and magnetic properties of IONPs. Several advantages were highlighted in this approach. Firstly, the procedure of dissolution and coating cannot be handled at harsh experimental conditions. Secondly, the coating process could be performed directly in water/pentane, avoiding the use of toxic solvents like DMSO and DMF. This reduction in toxic solvent usage minimized safety risks associated with their presence in trace amounts in final injectable solution. Lastly, the dendrimers modified with thermally unstable moieties under mild temperature. NPs can be conjugated with range of functional groups to enhance targeting and sensing. DLS analysis was used to assess the stability and average hydrodynamic diameter of NP-PAMAM NPs. The ease of application and versatility make it valuable for developing magnetic NPs for various biomedical applications, including as MR contrast agents [36]. The research conducted by Baccile, N., et al., gave details for the preparation of functional IONPs through both methods, utilizing natural functional glycolipid from sophorolipids (SL). These glycolipids, obtained through the fermentation process of the yeast Candida bombicola (Starmerella bombicola), offer an open acidic form highly conducive to nanoparticle stabilization. The resulting carbohydrate coated IONPs hold promise for biological applications, showcasing potential biocompatibility. The synthesis strategy allows for the tuning of magnetic properties, highlighting the influence of the glycolipid on structure of the final material, resulting in the formation of maghemite and ferrihydrite. Sophorolipids complex NP's surface were modified with carboxyl (COOH) groups to form stable colloids was revealed by various analytical techniques such as DLS, FTIR, UV-Vis. These colloids exhibit hydrodynamic diameters ranging from 10-30 nm in both 0.01M and 2M KCl solution and water. TEM micrographs and particle size distribution illustrate the spherical nature of the NPs, with sizes and homogeneity influenced. In particular, two step procedure, specifically 2S-RT and 2S-80C, yields particles with average diameters of 8.5 and 4.5 nm, respectively. The materials demonstrate smaller size distribution and stability when synthesized at 80 °C compared to room temperature. The NPs exhibit resilience through around 10 filtration steps, with aggregate size of approximately 100 nm. In summary, this research showcases the successful synthesis of functional IONPs using sophorolipids, emphasizing their potential for biomedical applications. The research provides a view into the NPs stabilization mechanism, tuning of magnetic properties, synthesis on stability and particle size. The findings contribute to the development of potentially biocompatible materials with applications in various biomedical fields [37].

Silica functionalization

Setyawan, H., et al., successfully prepared Silica-coated magnetite NPs through a single step electrochemical method. In this procedure, pure iron undergoes electrooxidation in a dilute aqueous sodium silicate solution, which serves as a silica precursor. The incorporation of silicate in the method proves to increase the purity of magnetite, whereas remove the impurities in the form of FeOOH which is usually found in magnetite prepared water. The magnetite NPs produced through the electrochemical approach exhibit a size range of 6 to 10 nm with spherical shape. The size of

prepared material was smaller as compared to the particles prepared in water, and it can be controlled by adjusting concentration of sodium silicate and voltage. The superparamagnetic NPs display high saturation magnetization in the range of 15-22 emu/g. while the saturation magnetization ofFe_3O_4 bulk material has higher value around 92 emu/g, the NPs remain superparamagnetic. The described electrochemical method presents a promising and facile synthetic route for the production of silica-coated magnetite NPs, offering control over particle size and demonstrating superparamagnetic properties [38]. In this study, Malvindi, M.A., et al., suggested that Fe_3O_4 coated with a thin silica shell (SiO_2) were investigated, and their surface passivation effects were explored using two different molecules: aminopropyltriethoxysilane (APTES) for positive surface charge and (trihydroxysilyl)-1-propanesulfonic acid (SIT) for negative surface charge. The structure of NPs contains Fe_3O_4 magnetic core which has a diameter of 12.0 ± 2.0 whereas SiO_2 make the shell with the thickness of 7.0 ± 1.5 nm. The combined core/shell structure of NPs gives the particle diameter of 26.0 ± 2.9 nm. Various analyses, including TEM, determine the size, shape, and coating thickness of the NPs. The study compared the bare Fe_3O_4/SiO_2 NPs with surface-passivated ones to assess the impact on the stability of particles as well as toxicity of particles. Cell toxicity of NPs were examined through reactive oxygen species (ROS) assays, cell viability, membrane integrity, mitochondrial membrane potential and genotoxicity. The results revealed that surface passivation significantly reduced oxidative stress, variation in iron homeostasis, and overall toxicity. Despite similar cell internalization efficiency, surface-passivated NPs exhibited lower toxicity compared to bare NPs. Specifically, bare NPs displayed substantial toxicity at higher concentrations, while passivated NPs, regardless of surface charge, demonstrated no signs of toxicity. A549 cells appeared to be more resistant to NP treatment overall. The study revealed that higher in-situ degradation enhanced the toxicity of bare NPs and as compared to surface-passivated NPs it releases iron ions in large quantity. The findings underscored the crucial role of surface engineering in enhancing the stability of Fe_2O_3/SiO_2 NPs in biotic environments, thereby decreasing cytotoxicity and genotoxicity effects [39]. Biodegradable lipid-coated polymeric NPs (LP) were determined for drug delivery for the co-encapsulation of doxorubicin (DOX) and CUR in the treatment of osteosarcoma (OS) were investigated by Wang, L., et al. The DOX + CUR LPNs were synthesized with biodegradable polymer core and mixed lipid monolayer shell. TEM images revealed that DOX+CUR LPNs had a size range of 100 nm with spherical shape and dark gray coats on darker spherical particles. The EE of DOX in DOX + CUR LPNs and DOX LPNs was approximately 85%, while the DEE of CUR was 80%. The zeta potential of DOX + CUR LPNs was measured at -33.4 mV. Free drug, single drug loaded LPNs and DOX+CUR LPNs were used to investigated cell cytotoxicity in mouse KHOS cell xenograft model also in human OS KHOS cell lines. DOX + CUR LPNs exhibited a more significant curative effect on OS cell lines compared to free drug molecules. Afterwards, animal model showed best anti-OS effects as compared to others. In vitro anti-OS efficacy assessed by MTT assay showed that the cytotoxicity of dual-drug-loaded LPNs was higher than single drug-loaded LPNs, and drug-loaded LPNs had enhanced cytotoxicity than free drug molecules. The IC50 values of All DOX + CUR LPNs showed lowest IC50 values than all other analyzed samples, indicating their enhanced efficacy. Furthermore, in vivo distribution analysis revealed that DOX and CUR distribution from DOX + CUR LPNs was greater in tumor tissues, potentially reducing side effects during tumor therapy. This dual-drug co-encapsulated LPNPs drug delivery system demonstrated promising results in enhancing drug delivery and activity against mice cancer cells and human OS cancer cells. The findings suggest potential new options for the treatment of osteosarcoma [40].

Carbon functionalization

Carbon has the capability to bind with all chemical elements therefore, it generates variety of compounds and molecules. Carbon has application in biomedical field for controlled pharmaceutical therapeutic agents, for drug delivery and sensing applications [41]. Wang, J., et al., conducted a research in which a bimorphological Fe_3O_4@C composite was synthesized using a chemical vapor deposition (CVD) method from Fe_2O_3 NPs, with acetylene serving as the deposition vapor and carbon source. The synthesis process led to the conversion of pristine Fe_2O_3 to Fe_3O_4, with the majority of particles recrystallizing into submicron octahedral Fe_3O_4 particles, while some remained as nano-sized particles. The Fe_3O_4 particles were coated carbon layer, with thicknesses ranging from 2 to 5 nm, resulting in a carbon content of 3wt%. As the deposition period was increased, the morphology of the composite evolved. After 20 minutes, the octahedral Fe_3O_4 particles further grew, and the number of nano-sized particles decreased. The Fe_3O_4 NPs were coated with 19% carbon layer with the thickness of 15-20 nm. Upon further increasing the deposition period to 30 minutes, 35% increases the carbon contains, accompanied with only carbon and generating iron carbides. Fe_3O_4@C composite can be prepared with deposition for about 20 minutes due to larger particle size which exhibited greater electrochemical properties. The reversible discharge capacity of 570 mAh/g at 100 mA/g, about 96% retention capacity after 60 cycles. Cycling performance including buffering volume changes, increasing electrical conductivity, and inhibit agglomeration of IO, improved by pyrolytic carbon. The larger size of the octahedral Fe_3O_4 particles also contributed to preventing accumulation during cycling. Fe_3O_4@C composite, have the submicron octahedral predominated with few nano spherical shaped particles. High-performance IO based anode materials for lithium-ion batteries (LIBs) [42]. The study revealed by Hadidi, L., et al., α-Fe_2O_3 nanorods, were synthesized by a new microwave-assisted method which coated with polydopamine through straightforward solution methods. The polydopamine-coated nanorods were then thermally treated in flowing argon to convert them into nitrogen-doped mesoporous carbon-coated (NDC) Fe_3O_4 nanorods. In the entire process, the morphological structure of the nanorods was preserved. The prepared hybrid material were explored for their potential used as catalysts for oxygen reduction reaction, shedding light on synergistic impact of the Fe_3O_4/NDC and significance of thickness of carbon shell. The α-Fe2O3 nanorods had a length of 141 nm ± 44.8 nm and diameters of 14 nm ± 3.4 nm. High-resolution TEM (HR-TEM) analysis confirmed the fringes with the nanorod long axis, consistent with the trigonal hexagonal structure of α-Fe_2O_3. The polydopamine coating was applied for varying times, resulting in different carbon shell thicknesses. The carbon content and thickness of the carbon shell were directly related to the coating time: 14.5 wt% with a thickness of 1.5 nm ± 0.2 nm for 2 hours, 20.8 wt% with a thickness of 2.2 nm ± 0.5 nm for 4 hours, and 38.3 wt% with a thickness of 3.5 nm ± 0.5 nm for 12 hours. The study revealed that the catalytic activity was influenced by the thickness of the nitrogen-doped carbon (ND-C) coating. Thick carbon layer, such as those in the 12-hour coating time sample, diminished catalyst effectiveness, likely due to the blocking of oxygen reduction reaction active sites on the Fe_3O_4 surface. Comparable or superior performance compared to commercial 40 wt% Pt-C catalyst were demonstrated by the optimal system, ND-Fe_3O_4@mC-2 (2 hr of coating time). It exhibited only 111 mV for superior limiting current density and more negative onset potential for oxygen reduction reaction [43]. Fe_3O_4 nanorods with carbon coating and pure Fe_3O_4 nanorods were prepared through a hydrothermal reaction followed by a frittage procedure introduced by Liu, J., et al. Characterization using SEM and XRD confirmed that the coating at carbon did not affect the morphology of Fe_3O_4. TEM revealed that the Fe_3O_4 nanorods were uniformly coated with a carbon

layer approximately 2 nm in thickness. The resulting Fe_3O_4/C nanorods had diameter size about 110 nm while length was approximately 510 nm. Carbon layers have the uniform and continuous characteristics plays vital role in enhancing electrochemical performance including (1) maintaining the probity of particles (2) enhancing electric conductivities. Electrochemical characteristics and features were investigated through various techniques galvanostatic charge-discharge cycling, electrochemical impedance spectroscopy, cyclic voltammetry. The Fe_3O_4/C nanorods exhibited enhanced electrochemical performance compared to pure Fe_3O_4. Specifically, a particular capacitance of 275.9 F g−1 was accomplished at a current density of 0.5 A g−1 in a 1 M Na_2SO_3 aqueous solution for Fe_3O_4/C nanorods, compared to 208.6 F g−1 for pure Fe_3O_4. The Fe_3O_4/C nanorods has the specific capacitance retention around 81.2% after 500 cycles. Fe_3O_4/C nanorods showed better cycling performance and higher specific capacitance. Overall, these results suggest that Fe3O4/C nanorods hold great potential as electrode materials for supercapacitors [44].

Antibodies/Antigens functionalization

The research discussed by Saei, A., et al., in the article focuses on a highly promising method for isolating tumor cells, which is used for early detection as well as prevent cancer cell mutations, also facilitate drug treatment and adjuvant therapies. The primary technique investigated the use of magnetic IONPs for immunomagnetic separation. The IONPs synthesized for this purpose were functionalized with antibodies targeting human epithelial growth factor receptor 2 (HER2). The receptor was known to be amplifying in various human cancer cells including 15% in breast cancer cell patients. The modification of IONPs with HER2-specific antibodies, referred to as Ab-IONPs, allows for the specific attachment of these NPs to HER2-positive cancer cells. This specificity makes Ab-IONPs highly efficient agents for the separation of individual cancer cells from fresh whole blood. The article provides detailed characterization of the synthesized NPs. DLS results revealed the particle size of IONPs and Ab-IONPs to be 84.9 nm and 328 nm, respectively. Inductively coupled plasma (ICP) analysis indicates an appropriate concentration of iron (1,564.5 ppm) in the coprecipitated IONPs, rendering them suitable for separation. The polydispersity index (PDI) values of IONPs and Ab-IONPs are reported as 0.104 and 0.350, respectively, providing insights into the distribution of particle sizes. Furthermore, IONPs have the presence of carboxyl groups and coat of citrate on the surface therefore it showed negative charge zeta potential with value of (-36.5 mV). The conjugation of IONPs with antibodies decreases the zeta potential -19.1 mV, attributed to the overall +ve charge of the antibodies. SEM images confirm the spherical morphology of IONPs before antibody conjugation. The successful attachment of magnetic IONPs to antibodies via 1-ethyl-3-(3-dimethylaminopropyl) carbodiimide/N-hydroxysuccinimide linkers is illustrated through the SEM results. Importantly, the study highlights the achieved specific targeting capability of the Ab-IONP complex. Specifically, 94.5 ± 0.8% efficiency is reported for the separation of BT474 HER2+ breast cancer cells, and 70.6 ± 0.4% capability is achieved for a mixed cell culture of BT474/MCF7. This high efficiency is noteworthy, especially considering the minimal amount of antibodies used, contributing to the economic viability of the proposed single-cell detection device. In summary, the research presents significant advancements in particle stability and cell separation efficiency compared to previous studies. The anti-HER2 monoclonal antibody conjugated IONPs successful showed the separation of HER2+ breast cancer cells. The accurate control of particle size and crystallinity during the synthesis process further contributes to the overall success of this innovative approach [45]. The study conducted by Rashid, Z., et al., focuses on the development of a magnetic activating cell sorting

(MACS) platform for the isolation of peripheral blood T CD4+ lymphocytes. The platform utilizes Fe_3O_4 magnetic NPs coated with a SiO_2 shell and further modified with N-(phosphonomethyl) iminodiacetic acid (PMIDA). Anti-CD4 monoclonal antibodies are then conjugated to the MNP surface for efficient isolation of T CD4+ lymphocytes. The synthesis of Fe_3O_4 NPs involves co-precipitation of Fe (III) and Fe (II) ions, followed by SiO_2 shell coating and PMIDA grafting. XRD analysis confirms the phase construction and the morphological crystallinity of the synthesized Fe_3O_4 and Fe_3O_4 @SiO_2@PMIDA MNPs. The mean particle sizes, calculated from XRD data, are 30 nm for Fe_3O_4 and 60 nm for Fe_3O_4@SiO_2@PMIDA, consistent with SEM images. SEM images reveal spherical-shaped Fe_3O_4 particles with an average diameter of around 30 nm. The modification of PMIDA on the surface of Fe_3O_4 NPs maintains the spherical shape but increases the average particle size to about 55–60 nm. To assess biocompatibility, the cell toxicity of Fe_3O_4@SiO_2@PMIDA MNPs was evaluated in vitro on peripheral blood mononuclear cells (PBMCs) isolated from whole blood. The results confirm the biocompatibility of the prepared MNPs. There was the activation of carboxylic modifications as covalent bindings between the EDC/ Fe_3O_4@SiO_2@PMIDA NHS with carboxylic groups on the MNPs and free amine sites of the antibodies. The immunomagnetic particles efficiently isolate T CD4+ lymphocytes from whole blood with high purity. The study demonstrates that the developed immunomagnetic NPs, through covalent binding with anti-CD4 antibodies, can specifically and efficiently purify T CD4+ cells from PBMCs. The MACS-based platform holds promise for applications in isolating healthy functional cells, particularly T CD4+ lymphocytes, in biomedical and clinical settings [46]. Bolandparvaz, A., et al., focuses on assessing the toxicity, biodistribution, and clearance of a therapeutical system for maternal autoantibody-related Maternal Autoantibody-Related (MAR) autism. The system involves ~15 nm citrate-coated dextran (DIONPs), surface-modified with PEG and MAR peptides, creating NP-based autoantibody reception and entrapment systems (SNAREs). The aim is to establish the security and feasibility of using SNAREs in pregnant murine dams. In vitro experiments assessed the immunogenicity and MAR lactate dehydrogenase B antibody uptake in murine serum. Minimum production of inflammatory cytokines (interleukin 10 and IL-12) was observed following macrophage exposure to SNAREs. In vivo study analyzed clinical trials and post-mortem pathological assessments were conducted to examine biodistribution, toxicity, and systemic effects. The maximum tolerated dose (MTD) of SNAREs was determined to be 150 mg/kg. Histological and magnetic resonance imaging analyses revealed iron deposition in the liver and lungs, but no evidence of associated organ damage, infection of lungs, or toxicity in liver was detectable. Furthermore, SNAREs expressed moderate clearance from blood of pregnant organism. Despite the retained in the blood, SNAREs were deemed secure in pregnant mice, showing no signs of inflammation, failure or damage of organ or any fetal mortality. The identification of the Maximum Tolerated Dose (MTD) lays the groundwork for future studies aimed at investigation the effectiveness of NPs formulation in a mouse model MAR autism. The findings suggest that SNAREs hold promise as a preventive therapeutic approach for MAR autism, pending further research on their efficacy in relevant models [47].

Natural Biomolecules functionalization

Now a days, natural product-based compounds leads for novel drug delivery. Natural products exhibit remarkable characteristics including chemical and biological properties, extraordinary chemical diversity, less toxicity, etc. Natural compounds used to screened or treat several major diseases, such as cardiovascular, inflammatory, cancer, microbial diseases, etc [48]. The study

presented by Gambhir, R.P., et al., introduces a novel method for extracting SARS-CoV-2 RNA using glycine-functionalized IONPs (G-IONPs). The key advantage of this approach lies in the pH-responsive nature of G-IONPs, making them highly efficient in the extraction process. The synthesis of these G-IONPs involves a one-pot co-precipitation method, which not only ensures high magnetic properties but also proves to be a cost-effective approach. The characterization of the synthesized G-IONPs is comprehensive and includes various analytical techniques. XRD analysis indicates the crystalline magnetite nature of the NPs, providing insights into their structural properties. FTIR and UV are employed to confirm the surface modification of the magnetic NPs with glycine. Morphological details are revealed through SEM and TEM, demonstrating a random composition and an average size of 20 nm for the G-IONPs. Importantly, TEM images depict similarities between the G-IONPs and bare IONPs, emphasizing the successful modification with glycine. The pH-responsive behavior of G-IONPs is attributed to the glycine availability as functionalization on their surface. In an acidic medium (pH < 7), glycine gains a positive surface charge, resulting in an overall positive charge on the G-IONPs. This positive charge facilitates the adsorption of RNA onto the surface of the NPs. Conversely, elution of RNA from G-IONPs was gained at pH=8 in basic medium, demonstrating the reversibility of the process. Further analyses involve vibrating sample magnetometer (VSM) and thermo-gravimetric analysis (TGA) to explore the magnetic and thermal properties of G-IONPs, respectively. The study reveals that glycine plays a crucial role as an RNA adsorbent, enabling efficient adsorption of SARS-CoV-2 RNA onto the G-IONPs under specific pH conditions (pH 6). The purity of the extracted RNA is assessed using UV–visible spectrometry. The efficiency of the RNA extraction process is confirmed through RT-PCR analysis, which detects the presence of SARS-CoV-2 specific genes (Envelope, RNA-dependent RNA polymerase, and Nucleocapsid). After 25 cycles of RT-PCR, it shows an increase in amount of genes that revealed RNA extraction by GIONPs. Additionally, agarose gel electrophoresis is employed to validate the quantity and quality of RNA extracted from SARS-CoV-2 patient samples. The study exhibited that in the extraction of SARS-CoV-2 RNA, GIONPs showed the reusability, due to repeated use of material in extraction. This aspect is crucial for practical applications, reveling the sustainability and robustness of the proposed method. In summary, the research signifies a significant advancement in the biomedical field for diagnosis of disease, particularly in the context of SARS-CoV-2. The innovative use of glycine-functionalized IONPs with pH-responsive properties offers an efficient and reversible method for RNA extraction. The study not only characterizes the synthesized G-IONPs comprehensively but also validates their efficacy through various analytical techniques and molecular assays, showcasing their potential as a promising tool for RNA extraction and disease detection [49]. The study conducted by Cojocaru, F.D., et al., describes the preparation of composites for potential applications in bone tissue engineering. These composites are formed by combining natural polymers such as gelatin, hyaluronic acid, CS, bovine serum albumin, calcium phosphate and magnetic NPs through co-precipitation method. The biomimetic approach mimics natural mineralization processes, in which polysaccharides, protein, polymers and many minerals combine together under physiological conditions. SEM analysis showed a macroporous morphology in the magnetic composites, influencing the retention of simulated biological fluids. FTIR, XRD, and EDX were employed to confirm the construction of the scaffolds and identify various types of amorphous calcium phosphates. The polymeric charged functional groups for nucleation centers for calcium phosphate includes amino groups from CS and COOH groups from hyaluronic acid. SEM micrographs demonstrated 3D structure with interconnected pores, housing both calcium phosphate crystals and MNPs homogenously within the polymeric matrix. EDX analysis confirmed the chemical composition of the magnetic scaffolds, revealing signals corresponding to

hydroxyapatite, other calcium phosphates, biopolymers, and MNPs. The studies related to in vitro trials indicated a low degradation mechanism for the magnetic composites, suggesting a strong connection between the calcium phosphates and polymeric matrix. It prevents the disintegration of the material by restricting the interaction of enzyme access to degradable components. The magnetic scaffolds demonstrated no negative effects on osteoblast cells, indicating good biocompatibility. Based on the properties observed, specific compositions involving 3% MNPs, calcium phosphates, CS, bovine serum albumin, hyaluronic acid were required for in vivo testing. Overall, these findings underscore the potential of the developed magnetic scaffolds for applications in bone tissue engineering, considering their favorable structure, composition, degradation characteristics, and biocompatibility [50]. Gordillo-Marroquín, C., et al., introduces a novel method for the detection of pulmonary tuberculosis (PTB) in sputum samples, comparing a MNPs-based colorimetric biosensing assay (NCBA) with traditional sputum smear microscopy (SSM). The NCBA utilizes glycan-functionalized (GMNP) to capture Mycobacterium tuberculosis (Mtb) cells in mucoid sputum samples, offering a cost-effective and accessible diagnostic approach for resource-limited environments. Experiments were conducted to optimize the NCBA, focusing on the concentration of GMNP and the digestion/decontamination solution. The study explored a combination of NaOH (0.4%) and N-acetyl-L-cysteine (NALC) (0.025–4%) in a 1:1 ratio for sputum digestion. The chosen concentration of NALC was crucial for achieving effective liquefaction without significantly increasing costs. The optimized NCBA, using 0.4% NaOH and 4% NALC, demonstrated a 143% increase in acid-fast bacilli (AFB) count compared to SSM, showcasing its superior performance. The glycan bioreceptor on GMNP facilitated the capture of Mtb cells in mucoid sputum samples, eliminating the need for expensive antibodies or aptamers. The carbohydrate-rich nature of the Mtb cell envelope allowed efficient binding with the glycan-functionalized NPs. The results indicated that NCBA not only increased the AFB count compared to SSM but also improved the grading from "1+" to "2+". This enhancement is particularly significant in paucibacillary cases, where a "scant" grade may elevate to "1+". The simplicity of the assay, utilizing a basic magnet and costing only $0.10 per test, makes it highly applicable in TB control programs, especially in resource-constrained settings. The NCBA technology, with its glycan-based magnetic isolation method, aligns well with the criteria for a rapid, affordable, and universally accessible TB test. The study suggests that implementing this technology in clinical practice has the potential to significantly enhance TB diagnosis and contribute to the global effort to reduce TB-related mortality. The proposed NCBA system stands out for its affordability, long shelf life, room-temperature storage, and easy preparation, making it a promising tool for improving TB diagnostics worldwide [51]. Arsalani, S., et al., research explained the ecofriendly synthesis of biocompatible MNPs with potential applications in various technological and biomedical fields. IONPs were prepared using coprecipitation technique at a moderate temperature, with natural rubber latex (NRL) extracted from Hevea brasiliensis serving as the capping agent. The use of a green approach is crucial for biomedical purposes to ensure biocompatibility. XRD patterns confirmed the spinel structure of the magnetic NPs, specifically magnetite Fe_3O_4. TEM images revealed that the core size of the MNPs could be managed by adjusting the concentration of NRL. The zeta potential measurements demonstrated that NRL-coated MNPs showed high colloidal stability as compared to uncoated MNPs. FTIR indicated the presence of OH groups in the uncoated MNPs, likely due to residual water at the MNP surface. DLS measurements provided insights into the hydrodynamic sizes of only MNPs and NRL-coated MNPs after washing. The NRL-coated MNPs showed enhanced colloidal stability, as evidenced by the hydrodynamic size measurements. TEM images and size distribution histograms revealed spherical-shaped NPs for all samples. The average core sizes varied

with the amount of NRL, estimated to be 12±4 nm for bare MNPs, 13±2.8 nm for NRL-100, 10.3±2.2 nm for NRL-400, and 7.9±1.5 nm for NRL-800 MNPs. The zeta potential of the suspensions further indicated effective stabilization by NRL, with positive values for NRL-coated MNPs compared to the negative zeta potential of bare MNPs. Hall magnetometer measurements demonstrated that the IONPs exhibited superparamagnetic behavior, with NRL-coated NPs showing higher magnetization than the bare MNPs. This suggests that NRL effectively stabilizes the MNPs, making them suitable for biomedical applications. In conclusion, the study highlights the effectiveness of NRL as a stabilizing agent for M NPs, offering a green and biocompatible synthesis approach. The resulting NRL-coated MNPs exhibit enhanced stability and magnetization, making them promising candidates for biomedical applications [52]. The study by Liu, P., et al., focuses on the critical step of harvesting oleaginous microalgae for biodiesel production, utilizing Fe_3O_4 magnetic NPs modified with amino acid for enhanced properties, economical, and convenient operation. Synthesis techniques included thermal decomposition and chemical co precipitation for Fe_3O_4 NPs were compared, and for amino acid modification three techniques can be used including long-time mixing, ultrasonic and one-step. The investigation primarily targeted the harvesting of oleaginous microalgae Chlorella sp. HQ. The results revealed that Fe_3O_4 NPs prepared through chemical coprecipitation method outperformed the thermal decomposition method in terms of both harvesting efficiency and fabrication cost. The average sizes of the Fe_3O_4 NPs were 17.83 nm and 14.44 nm for thermal decomposition and chemical coprecipitation, respectively. TEM images illustrated polydisperse Fe_3O_4 NPs with average particle sizes of 13.30 nm and 12.16 nm for thermal decomposition and chemical coprecipitation, respectively, consistent with values calculated from XRD. For the modification of amino acid step, the "one-step" approach proved to be more effective than ultrasonic and long-time mixing methods. Optimized Fe_3O_4@Arginine NPs, with a dosage of 200 mg/L, achieved a harvesting efficiency of 95% at a relatively economical cost of 347 USD per ton of harvested algal biomass. The number of amino groups present inside the amino acid molecule and the number of amino acid consist on the surface of NPs were identified as factors contributing to improved harvesting performance. The study demonstrates the importance of optimizing synthesis methods and modification approaches for Fe_3O_4 MNPs in the harvesting of oleaginous microalgae. The use of amino-acid-modified Fe_3O_4 NPs, particularly with the "one-step" approach, showcases promising results in terms of harvesting efficiency and low budget, making it a potential method for wide-range biodiesel production from microalgae [53]. Bani, M.S., S. Hatamie, and M. Haghpanahi, investigates the use of casein-coated MNPs as a heat generation source for cancer hyperthermia therapy, with a focus on biocompatibility and in vivo performance. IONPs are commonly employed for magnetic hyperthermia, and surface enhancements, such as casein coating, are explored to improve performance while evaluating cytotoxicity for biomedical applications. In cell viability tests, normal cell lines-maintained viability above 95% at 0.5 and 1 mg/mL concentrations, with the minimum recorded viability at 84.78% for normal cell lines at a 20 mg/mL concentration. In contrast, cancer cell lines in contact with casein-coated NPs showed reduced viability, with most samples less than 85%. Samples with lower NPs concentration (~20-30% drops) were shown decrease in cell viability by introducing the change in magnetic field, while higher concentrations experienced a ((~10-20%) decrease. In vivo trials demonstrated a 33% reduction in tumor size after just 1 week of hyperthermia treatment with casein-coated NPs. The viability of cancer cell lines decreased with increasing NP concentration, with significant changes observed over time. The utmost recorded viability for 4T1 and MCF7 cell lines was 83.99% and 85.88%, respectively, at a 0.5 mg/mL sample, whereas the lowest viability was 70.18% and 70.13% for the highest NP concentration. Real-time polymerase chain reaction (PCR)

outcome confirmed the effectiveness of the hyperthermia treatment. Furthermore, the study suggests that a core-shell morphology influences tumor growth, combining better biocompatibility, inherent hostility toward cancer cells, and efficient heating power. Lower injection speeds were proposed to improve NP distribution and treatment efficacy. Overall, the findings indicate the potential of casein-coated NPs for hyperthermia cancer therapy applications, offering a combination of biocompatibility, selective cytotoxicity towards cancer cells, and effective heating power [54].

Folic acid functionalization

In this study conducted by Wang, Y., et al., a micelle system introduced, synthesis of folic acid modified succinylated gelatin (FA-SG) and utilization as a drug carrier for folate-receptor(FR) for antitumor therapy.
FA-SG copolymer was characterized by fluorescence spectroscopy and 1H NMR. Subsequently, dialysis method was used to synthesize doxorubicin-loaded FA-SG (DOX-FA-SG) micelle and TEM analysis confirmed it's spherical shaped morphology. The average diameter of DOX-FA-SG micelles was measured to be 277 nm, with a DOX-loading content of 12.4%. The zeta potential value of blank and DOX-loaded micelles ranged from −7.42 to −1.42 mV. In vitro drug release profile showed a sustained release over 168h for DOX-loaded micelles.
The DOX-FA-SG micelles showed cytotoxicity again FR-positive MCF-7 cells than DOX-loaded micelles and it also showed increased cellular uptake as well. Notably, DOX-FA-SG micelles exhibited greater activity against MCF-7 tumor cells in mice as compared to DOX-loaded micelles without FA and DOC.HCl. In summary, FA-SG micelles were identified as successful carriers for targeted drug delivery, showcasing enhanced cellular uptake and antitumor efficacy, particularly in FR-positive cancer cells and mouse models. The study suggests the potential of FA-SG micelles in targeted cancer therapy. MCF-7 and A549 cell lines were used to observe stronger fluorescence of DOX following incubation with DOX.HCl than DOX-FA-SG and DOX-SG micelles. This observation revealed that DOX-FA-SG micelles may have different kinetic properties and cellular uptake [55]. Research conducted by Nemati, M., et al., explained FA-CS NPs were synthesized using various concentrations (5, 10, and 20%) of FA. The NPs were unveil to plasmas from healthy donors and breast cancer patients to investigate the formation of a protein corona and its potential effects on delivery capacity. The study focused on evaluating the interaction between the NPs and biological components, especially in the context of personalized medicine. The establishment of protein corona around FA-CS NPs resulted in changes in their physicochemical properties, including an increase in NPs size and a shift towards a more -ve surface charge. The difference between the content and type of plasma protein functionalized to NP surface was revealed by SDS-PAGE electrophoresis. The formation of the protein corona was found to be personalized, varying between breast cancer patients and healthy donors. The composition of PC did not induce cytotoxic effects on breast cancer cells (MDA-MB-231); however, it led to a reduction in nanoparticle uptake efficiency. The formation of the biological environment, specifically the patients' plasma may reduce cellular internalization rate and uptake of NPs. Raw264.7 cells, representing monocyte/macrophage-like cells, showed efficient adsorption of both bare and protein corona-coated NPs, suggesting ligand–receptor-dependent and independent cellular engulfment. Patients' sera were observed an specific behavior and observed an approach for the targeted delivery of biomolecules in immune system disorders. The study emphasizes the personalized nature of the protein corona, with implications for the delivery efficiency of FA-CS NPs in breast cancer patients. It suggests that the PC-coated NPs may find applications in delivering

particular biomolecules in immune system disorders [56]. In this research, Yücel, O., et al., focused on developing an advanced drug delivery system using AuNPs as the carrier. The key objective was intensifying the pharmaceutical efficiency and decrease potential toxicity by incorporating targeting mechanisms into the delivery system. The approach involved coating the AuNPs with glutathione (GSH) and modifying them with folate (FA), a vitamin that has been found to interact with folate receptors commonly overexpressed in certain cancer cells. The synthesis process resulted in the development of spherical AuNPs with a size of 5.6 nanometers. These NPs were initially coated with GSH and subsequently modified with FA, leading to the creation of Au-GSH-FA NPs. The next step involved loading the anticancer drug methotrexate (MTX) onto these NPs, resulting in larger particle size approximately 11 nm. The careful characterization of these NPs was conducted using DLS and TEM to confirm their morphology, size distribution, and stability. The significance of incorporating folate into the system lies in its ability to bind to folate receptors, which are often overexpressed on the surfaces of certain cancer cells. This targeting strategy aims to improve the delivery of drug to the specific unhealthy cells or cancer cell and preventing healthy cells from the drug side effects. In vitro studies were conducted to evaluate the performance of the MTX-loaded NPs (MTX/Au-GSH-FA). The results revealed a substantial increase in cytotoxicity against folate receptor-positive cancer cells, specifically those from human brain (U-87 MG) and cervical (HeLa) cancers, when compared to the free form of MTX. Importantly, the cytotoxic effect was minimal in folate receptor-negative human cell lines, emphasizing the specificity of the delivery system. The findings were further supported by fluorescent microscopic imaging, confirming the receptor-specific uptake of the MTX/Au-GSH-FA NPs by cancer cells. In conclusion, this research showcases the successful evolution of a targeted drug delivery system using AuNPs functionalized with glutathione and folate. The system exhibited enhanced efficacy in delivering methotrexate to folate receptor-positive cancer cells, highlighting its potential as a promising approach for targeted cancer treatment [57]. The primary aim of the research conducted by Rahmati, A., et al., was to fabricate NPs composed of α-terpineol (αT) and PLGA, further coated with αT-PCF-NPs, and to assess their anticancer effects. The synthesis of αT-PCF-NPs was achieved using the nanoprecipitation technique, and various characterizations, including DLS, zeta potential, SEM, and FTIR, were conducted. HPLC were used to quantify entrapment efficiency and FA binding rate for α-T. The cytotoxicity of αT-PCF-NPs was evaluated through MTT assays, and pro-apoptotic properties were assessed using quantitative polymerase chain reaction (qPCR) analysis, acridine orange and propidium iodide (AO/PI) staining, and cell cycle analysis. The results indicated a successful synthesis of αT-PCF-NPs with a particle size of 263.95 nm, a polydispersity index (PDI) of 0.25, and a surface charge of +38.20 mV. The FA-binding rate and encapsulation efficiency of α-T were reported to be 67% and 88.1%, respectively. Importantly, αT-PCF-NPs exhibited a higher inhibitory effect on cancer cells compared to human foreskin fibroblast (HFF) cells, confirming their selective cytotoxicity. The pro-apoptotic effects of αT-PCF-NPs were evidenced by an increase in SubG1 phase cells, AO/PI staining results, and the modulation of pro and anti-apoptotic genes (Bax and Bcl-2) in HT-29 cells. Furthermore, αT-PCF-NPs demonstrated inhibitory effects on antioxidant (SOD) and angiogenesis-related genes (VEGF and VEGF-R) in HT-29 cells. In a murine colon cancer model, exposure to αT-PCF-NPs resulted in a significant reduction in tumor size, confirming their potential as an effective anticancer drug for colon cancer. Overall, these findings suggest that αT-PCF-NPs act as target specific and therapeutic approach for colon cancer treatment [58]. Mariadoss, A.V.A., et al., research aimed to synthesize copper oxide NPs (CuO) using extracts from Helianthus tuberosus (Ht), followed by encapsulation with starch (ST) and conjugation with FA to enable targeted release in MDA-MB-231 cells. The

resulting NPs, named FA-ST-HtCuONPs, were confirmed by DLS and TEM characterization techniques revealing hexagonal, oval-shaped particles with an average size of approximately 108.83 nm and a zeta potential of 43.26 mV. The optimized formulation with a ratio of 1:5 exhibited an mean particle size of 148.33 nm, a polydispersity index (PDI) value of 0.215, and a zeta potential of -35.29 mV. NPs have the presence of various functional derivatives including FA, starch and phytochemicals by FTIR characterization. UV indicated the accumulation of approximately 241.25 nmol/mg of FA on the surface of FA-ST-HtCuONPs. The Debye-Scherrer equation determined nanocrystalline sizes of 27.93 nm and 21.07 nm for HtCuONPs and FA-ST-HtCuONPs, respectively. TEM and SEM revealed a size distribution of HtCuONPs ranging from 24.93 to 275.41 nm, with an average particle size of 121.91 nm. Cytotoxicity assays demonstrated that FA-ST-HtCuONPs exhibited higher cytotoxicity (IC50 of 21.03 ± 1.85 µg/mL) against human breast cancer (MDA-MB-231) cells. This effect was assigned to activate ROS generation, reduction of mitochondrial membrane potential, modulation of apoptosis-related protein expression and nuclear damage. The outcomes underscored the role of FA and starch decoration in enhancing NPs insertion in cells through FR-based endocytosis, suggesting the potential of FA-ST-HtCuONPs for improved breast cancer therapy [59]. The research conducted by Law, S., A.W. Leung, and C. Xu, introduced a targeted drug delivery system for celastrol, a traditional Chinese medicine used as anticancer drug, was developed to address its low water solubility and lack of tumor selectivity. AuNPs were initially conjugated with PVP-co-2-dimethylaminoethyl methacrylate (Polymer) and celastrol, and the resulting complex was further modified with FA. The synthesized FR-targeted celastrol AuNP (FCA) was thoroughly characterized using various techniques. The mean size of the as-prepared AuNP was found to be 20.02 ± 4.70 nm. After conjugation with PVP-co-2-dimethylaminoethyl methacrylate and FA, the sizes of CA and FCA slightly increased to around 21.45 ± 4.76 nm and 22.00 ± 4.48 nm, respectively. FCA exhibited good solubility, high encapsulation efficiency (90%), and loading content (50%). There was a rapid release of drug within the initial 12 hrs, whereas at pH 5sustained release was observed after 72 hrs. FCA demonstrated high cellular uptake and significant inhibition of breast cancer cells in both 2D and 3D models. The interaction between the quinone methide chromophore group of celastrol and the surface plasmon resonance of AuNPs played a crucial role in the formulation. FCA induced more substantial apoptosis compared to celastrol AuNP and celastrol alone in both models. The sustain drug release observed at 12 and 72 hours was 80.18% and 82.46%, indicating sustained release. However, the cumulative release at pH 6.8 and pH 7.4 was lower, suggesting that celastrol in FCA remained within the AuNPs shell. Overall, FCA demonstrated improved water solubility and increased toxicity against breast cancer cells, making it a potential candidate for further development as an anticancer drug for breast cancer treatment [60]. Alirezaei, M., M. Ghobeh, and A. Es-haghi, introduced a targeted drug delivery system was developed using PLGA NPs coated with CS conjugated FA for the encapsulation of Artemisia vulgaris L. essential oil (AVEO). The physicochemical properties of the resulting AVEO-loaded PLGA-CS-FA (AVEO-PCF-NPs) were thoroughly characterized using various techniques. DLS analysis revealed that AVEO-PCF-NPs exhibited a spherical shape with dimensions below 300 nm, which was further supported by SEM images. FTIR confirmed the successful coating of CS and conjugation of FA on the NP surface. HPLC was employed to quantify the encapsulation of AVEO and the binding of FA. The anticancer effects of AVEO-PCF-NPs were evaluated through multiple assays. MTT assays demonstrated a significant suppression of cancer cells with an IC50 of approximately 78 µg/ml, while normal cells remained unaffected. Flow cytometry analysis and acridine orange/propidium iodide staining indicated pro-apoptotic effects, revealing cell arrest in the SubG1 phase. Furthermore, the chorioallantoic membrane (CAM) assay demonstrated the obstacle for AVEO-PCF-NPs on

angiogenesis, with a significant reduction in blood vessel formation. The inhibition rate increased with higher concentrations of AVEO-PCF-NPs, reaching about 20% at 50 µg/ml, and the most restrictive effect against cancer cells was observed at 100 µg/ml. These findings highlight the selective toxicity, apoptotic-inducing potential, and anti-angiogenic properties of AVEO-PCF-NPs, positioning them as a promising candidate for further research in cancer therapy. The targeted drug delivery system demonstrated its potential in enhancing the efficacy of AVEO against cancer cells while minimizing adverse effects on normal cells [61]. Maity, S., et al., focused on the chemical synthesis of polymeric NPs as a biofriendly delivery vehicle for enhancing the solubility of the flavanone naringenin in an antidiabetic animal study. The NPs were synthesized using two low-cost carbohydrate biopolymers, CS, and alginate, for the successful entrapment of naringenin. Dual crosslinked NPs were prepared using $CaCl_2$ and Na_2SO_4 as crosslinkers. The characterization of NPs involved techniques such as DLS, FTIR, XRD, and SEM. NPs hydrodynamic size was observed around 150-300 nm while the surface charge ratio was around -26.3- -38.21 mV. The optimal ration for CS:Alginate was 2:1 and 3:1, whereas the with size range of approximately 224.58 ± 11 nm and 216.44 ± 06 nm. It also showed minimum polydispersity index. The presence of alginate as an out layer of the core-shell NPs were confirmed by highly negative value for zeta potential. Different weight ratios were observed for naringenin loading capacity of CS/ALG core-shell NPs which were in between 7.41% and 19.87% with 57.34% and 98.36% was encapsulation efficiency. The synthesized nano-formulations demonstrated notable naringenin entrapment (>90%) and retained the sustain flavonoid release with pH-sensitive effect. In vivo studies declared that oral delivery of NPs showed notably hypoglycemic effects to streptozotocin-induced diabetic rats. Oral administration of NPs were considered as non-toxic by histopathology and various blood parameters. The polymeric formulation of naringenin as therapeutic oral delivery was considered as effective for various treatments such as hyperglycemia, hemoglobin iron-mediated oxidative stress in type 1 diabetic and dyslipidemia [5].

Conclusion

Nanomaterials can be used to deliver drug at a specific site and act as a carrier. There are various methods that you be used to make them target specific. Surface functionalization plays a vital role in making the nanocarriers target specific. In this regard, the surfaces of nanomaterials are usually functionalized with some antigen or other compound that could be an anti-body, which will direct the nanocarriers through injected body and bring them to a specific target and lets them deliver drug where it is required.

References

1. Sesarman, A., et al., *Co-delivery of curcumin and doxorubicin in PEGylated liposomes favored the antineoplastic C26 murine colon carcinoma microenvironment.* Drug Delivery and Translational Research, 2019. **9**(1): p. 260-272.

2. Jin, H.-H., Q. Lu, and J.-G. Jiang, *Curcumin liposomes prepared with milk fat globule membrane phospholipids and soybean lecithin.* Journal of Dairy Science, 2016. **99**(3): p. 1780-1790.
3. Bouarab, L., et al., *Influence of lecithin–lipid composition on physico-chemical properties of nanoliposomes loaded with a hydrophobic molecule.* Colloids and Surfaces B: Biointerfaces, 2014. **115**: p. 197-204.
4. Majumdar, D., et al., *Luteolin nanoparticle in chemoprevention: In vitro and in vivo anticancer activity.* Cancer Prevention Research, 2014. **7**(1): p. 65-73.
5. Maity, S., et al., *Alginate coated chitosan core-shell nanoparticles for efficient oral delivery of naringenin in diabetic animals—An in vitro and in vivo approach.* Carbohydrate Polymers, 2017. **170**: p. 124-132.
6. Li, Y., et al., *Dual Stable Nanomedicines Prepared by Cisplatin-Crosslinked Camptothecin Prodrug Micelles for Effective Drug Delivery.* ACS Applied Materials & Interfaces, 2019. **11**(23): p. 20649-20659.
7. Wang, X., et al., *NANOROBOTS: Intracellular manipulation and measurement with multipole magnetic tweezers.* Science Robotics, 2019. **4**(28).
8. Battistella, C. and H.A. Klok, *Controlling and Monitoring Intracellular Delivery of Anticancer Polymer Nanomedicines.* Macromolecular Bioscience, 2017. **17**(10).
9. Germain, M., et al., *Delivering the power of nanomedicine to patients today.* Journal of Controlled Release, 2020. **326**: p. 164-171.
10. Alshehri, S., et al., *Progress of Cancer Nanotechnology as Diagnostics, Therapeutics, and Theranostics Nanomedicine: Preclinical Promise and Translational Challenges.* Pharmaceutics, 2021. **13**(1): p. 24.
11. Sanità, G., B. Carrese, and A. Lamberti, *Nanoparticle surface functionalization: how to improve biocompatibility and cellular internalization.* Frontiers in molecular biosciences, 2020. **7**: p. 587012.
12. Hassan, S.-u. and X. Zhang, *Droplet-based microgels: Attractive materials for drug delivery systems.* Res. Dev. Mater. Sci, 2019. **11**: p. 1183-1185.
13. Begines, B., et al., *Polymeric nanoparticles for drug delivery: Recent developments and future prospects.* Nanomaterials, 2020. **10**(7): p. 1403.
14. Ahmed, H., et al., *Biomedical applications of mesoporous silica nanoparticles as a drug delivery carrier.* Journal of Drug Delivery Science and Technology, 2022. **76**: p. 103729.
15. Kumari, P., B. Ghosh, and S. Biswas, *Nanocarriers for cancer-targeted drug delivery.* Journal of drug targeting, 2016. **24**(3): p. 179-191.
16. Punitha, N., et al., *Antifouling activities of β-cyclodextrin stabilized peg based silver nanocomposites.* Applied Surface Science, 2017. **392**: p. 126-134.
17. Kumar, V., et al., *Nanomedicine-based approaches for delivery of herbal compounds.* Tradit Med Res, 2022. **7**(5): p. 48.
18. Gonzalez-Pech, N. and V. Grassian, *Surface chemical functionalities of environmental nanomaterials.* 2018.
19. Popescu, C., et al., *An experimental study on nano-carbon films as an anti-wear protection for drilling tools.* Coatings, 2017. **7**(12): p. 228.
20. Wu, Q., H. Lv, and L. Zhao, *Applications of carbon nanomaterials in chiral separation.* TrAC Trends in Analytical Chemistry, 2020. **129**: p. 115941.

21. Anwar, A., et al., *Advanced glycation endproducts, dityrosine and arginine transporter dysfunction in autism - A source of biomarkers for clinical diagnosis.* Molecular Autism, 2018. **9**(1).
22. Khameneh, B., et al., *Review on plant antimicrobials: a mechanistic viewpoint.* Antimicrobial Resistance & Infection Control, 2019. **8**(1): p. 1-28.
23. Martínez-Pérez, E.F., et al., *Natural Antispasmodics: Source, Stereochemical Configuration, and Biological Activity.* BioMed Research International, 2018. **2018**.
24. Salehi, B., et al., *Resveratrol: A double-edged sword in health benefits.* Biomedicines, 2018. **6**(3).
25. Gil, A.A.P., et al., *Anti-inflammatory and antinociceptive activities of the ethanolic extract of Bougainvillea xbuttiana.* Journal of Ethnopharmacology, 2012. **144**(3): p. 712-719.
26. Elkordy, A.A., et al., *An overview on natural product drug formulations from conventional medicines to nanomedicines: Past, present and future.* Journal of Drug Delivery Science and Technology, 2021. **63**: p. 102459.
27. Ayyanaar, S., et al., *Iron oxide nanoparticle core-shell magnetic microspheres: Applications toward targeted drug delivery.* Nanomedicine: Nanotechnology, Biology and Medicine, 2020. **24**: p. 102134.
28. Mansourizadeh, F., et al., *Designing Salvigenin –loaded mPEG-b-PLGA @Fe3O4 nanoparticles system for improvement of Salvigenin anti-cancer effects on the breast cancer cells, an in vitro study.* Journal of Drug Delivery Science and Technology, 2020. **57**: p. 101619.
29. Ahmed, A., et al., *pH and ultrasound dual-responsive drug delivery system based on PEG–folate-functionalized Iron-based metal–organic framework for targeted doxorubicin delivery.* Colloids and Surfaces A: Physicochemical and Engineering Aspects, 2021. **626**: p. 127062.
30. Sampath, M., et al., *The remarkable role of emulsifier and chitosan, dextran and PEG as capping agents in the enhanced delivery of curcumin by nanoparticles in breast cancer cells.* International Journal of Biological Macromolecules, 2020. **162**: p. 748-761.
31. Kommareddy, S. and M. Amiji, *Poly(ethylene glycol)–modified thiolated gelatin nanoparticles for glutathione-responsive intracellular DNA delivery.* Nanomedicine: Nanotechnology, Biology and Medicine, 2007. **3**(1): p. 32-42.
32. Norouzi, M., et al., *Salinomycin-Loaded Iron Oxide Nanoparticles for Glioblastoma Therapy.* Nanomaterials, 2020. **10**(3): p. 477.
33. 33. Wu, Y., et al., *Surface Modification of Iron Oxide-Based Magnetic Nanoparticles for Cerebral Theranostics: Application and Prospection.* Nanomaterials, 2020. **10**(8): p. 1441.
34. Barenholz, Y., *Doxil® — The first FDA-approved nano-drug: Lessons learned.* Journal of Controlled Release, 2012. **160**(2): p. 117-134.
35. Sintov, A.C., *AmyloLipid Nanovesicles: A self-assembled lipid-modified starch hybrid system constructed for direct nose-to-brain delivery of curcumin.* International Journal of Pharmaceutics, 2020. **588**: p. 119725.
36. Boni, A., et al., *Water dispersal and functionalization of hydrophobic iron oxide nanoparticles with lipid-modified poly (amidoamine) dendrimers.* Langmuir, 2013. **29**(35): p. 10973-10979.
37. Baccile, N., et al., *Sophorolipids-functionalized iron oxide nanoparticles.* Physical Chemistry Chemical Physics, 2013. **15**(5): p. 1606-1620.
38. Setyawan, H., et al., *One-step synthesis of silica-coated magnetite nanoparticles by electrooxidation of iron in sodium silicate solution.* Journal of Nanoparticle Research, 2012. **14**(4): p. 807.

39. Malvindi, M.A., et al., *Toxicity assessment of silica coated iron oxide nanoparticles and biocompatibility improvement by surface engineering.* PloS one, 2014. **9**(1): p. e85835.
40. Wang, L., et al., *The effective combination therapy against human osteosarcoma: doxorubicin plus curcumin co-encapsulated lipid-coated polymeric nanoparticulate drug delivery system.* Drug delivery, 2016. **23**(9): p. 3200-3208.
41. Zhao, Q., et al., *Spectroscopic studies of the optical properties of carbon dots: recent advances and future prospects.* Materials Chemistry Frontiers, 2020. **4**(2): p. 472-488.
42. Wang, J., et al., *Chemical vapor deposition prepared bi-morphological carbon-coated Fe3O4 composites as anode materials for lithium-ion batteries.* Journal of Power Sources, 2015. **282**: p. 257-264.
43. Hadidi, L., et al., *Microwave-assisted synthesis and prototype oxygen reduction electrocatalyst application of N-doped carbon-coated Fe3O4 nanorods.* Nanotechnology, 2017. **28**(9): p. 095707.
44. Liu, J., et al., *Synthesis of carbon-coated Fe 3 O 4 nanorods as electrode material for supercapacitor.* Ionics, 2013. **19**: p. 1255-1261.
45. Saei, A., et al., *Antibody-modified magnetic nanoparticles as specific high-efficient cell-separation agents.* Journal of Biomedical Materials Research Part B: Applied Biomaterials, 2020. **108**(6): p. 2633-2642.
46. Rashid, Z., et al., *Surface modification and bioconjugation of anti-CD4 monoclonal antibody to magnetic nanoparticles as a highly efficient affinity adsorbent for positive selection of peripheral blood T CD4+ lymphocytes.* International Journal of Biological Macromolecules, 2020. **161**: p. 729-737.
47. Bolandparvaz, A., et al., *Biodistribution and toxicity of epitope-functionalized dextran iron oxide nanoparticles in a pregnant murine model.* Journal of Biomedical Materials Research Part A, 2020. **108**(5): p. 1186-1202.
48. Chemat, F., et al., *A review of sustainable and intensified techniques for extraction of food and natural products.* Green Chemistry, 2020. **22**(8): p. 2325-2353.
49. Gambhir, R.P., et al., *pH-responsive glycine functionalized magnetic iron oxide nanoparticles for SARS-CoV-2 RNA extraction from clinical sample.* Journal of Materials Science, 2022. **57**(28): p. 13620-13631.
50. Cojocaru, F.D., et al., *Biopolymers – Calcium phosphates composites with inclusions of magnetic nanoparticles for bone tissue engineering.* International Journal of Biological Macromolecules, 2019. **125**: p. 612-620.
51. Gordillo-Marroquín, C., et al., *Magnetic Nanoparticle-Based Biosensing Assay Quantitatively Enhances Acid-Fast Bacilli Count in Paucibacillary Pulmonary Tuberculosis.* Biosensors, 2018. **8**(4): p. 128.
52. Arsalani, S., et al., *Green Synthesis and Surface Modification of Iron Oxide Nanoparticles with Enhanced Magnetization Using Natural Rubber Latex.* ACS Sustainable Chemistry & Engineering, 2018. **6**(11): p. 13756-13765.
53. Liu, P., et al., *Effects of Fe3O4 nanoparticle fabrication and surface modification on Chlorella sp. harvesting efficiency.* Science of The Total Environment, 2020. **704**: p. 135286.
54. Bani, M.S., S. Hatamie, and M. Haghpanahi, *Biocompatibility and hyperthermia cancer therapy of casein-coated iron oxide nanoparticles in mice.* Polymers for Advanced Technologies, 2020. **31**(7): p. 1544-1552.

55. Wang, Y., et al., *Preparation and evaluation of folic acid modified succinylated gelatin micelles for targeted delivery of doxorubicin.* Journal of Drug Delivery Science and Technology, 2018. **46**: p. 400-407.
56. Nemati, M., et al., *Unraveling the Effect of Breast Cancer Patients' Plasma on the Targeting Ability of Folic Acid-Modified Chitosan Nanoparticles.* Molecular Pharmaceutics, 2021. **18**(12): p. 4341-4353.
57. Yücel, O., et al., *Folic acid-modified methotrexate-conjugated gold nanoparticles as nano-sized trojans for drug delivery to folate receptor-positive cancer cells.* Nanotechnology, 2020. **31**(35): p. 355101.
58. Rahmati, A., et al., *Fabrication and assessment of folic acid conjugated-chitosan modified PLGA nanoparticle for delivery of alpha terpineol in colon cancer.* Journal of Biomaterials Science, Polymer Edition, 2022. **33**(10): p. 1289-1307.
59. Mariadoss, A.V.A., et al., *Folic acid functionalized starch encapsulated green synthesized copper oxide nanoparticles for targeted drug delivery in breast cancer therapy.* International Journal of Biological Macromolecules, 2020. **164**: p. 2073-2084.
60. Law, S., A.W. Leung, and C. Xu, *Folic acid-modified celastrol nanoparticles: synthesis, characterization, anticancer activity in 2D and 3D breast cancer models.* Artificial Cells, Nanomedicine, and Biotechnology, 2020. **48**(1): p. 542-559.
61. Alirezaei, M., M. Ghobeh, and A. Es-haghi, *Poly(lactic-co-glycolic acid)(PLGA)-based nanoparticles modified with chitosan-folic acid to delivery of Artemisia vulgaris L. essential oil to HT-29 cancer cells.* Process Biochemistry, 2022. **121**: p. 207-215.